#048

A millennium of loading: Paleoseismically constrained Coulomb stress evolution on the Carrizo and Coachella segments of the San Andreas Fault

Liliane Burkhard[1,2] and Bridget R. Smith-Konter[2,3]

[1] Space Research & Planetology Division, Physics Institute, University of Bern, Switzerland, liliane.burkhard@unibe.ch
[2] Dept. of Earth Sciences, University of Hawai'i at Manoa, liliane@hawaii.edu
[3] Northern Arizona University, Flagstaff, AZ, bridget.konter@nau.edu

Abstract

The Carrizo and Coachella segments represent two of the most consequential locked sections of the San Andreas Fault System (SAFS), having last ruptured in 1857 and ~1726, respectively. While contemporary geodesy tightly constrains present-day strain accumulation, the absolute stress state of these segments reflects the cumulative effects of multiple earthquake cycles, postseismic relaxation and fault network interactions. We integrate GNSS- and InSAR-constrained slip rates and locking depths with a millennial-scale paleoseismic rupture chronology (Maximum Rupture Model; Scharer & Yule, 2020) in a high-resolution 4D semi-analytic viscoelastic earthquake cycle model (maxwell) to reconstruct Coulomb stress evolution along the SAF System from 1000-2026 CE. Prescribed ruptures release accumulated slip deficit while deep slip beneath locked segments drives secular loading; stresses are evaluated at half the local locking depth. The Carrizo segment (~36 mm/yr; 18.7 km locking depth) exhibits quasi-periodic stress cycles punctuated by eight ruptures since ~975 CE, with pre-rupture thresholds of 0.5-3.9 MPa. Present-day stress (~3.3 MPa) exceeds the mean pre-rupture threshold (~1.3 MPa), placing this segment in a relatively advanced stage of its earthquake cycle despite a moderate stress accumulation rate (1.9 MPa/100 yr). The Coachella segment (~20 mm/yr; 11.5 km locking depth) shows repeated cycles with consistent ~2 MPa pre-rupture thresholds, yet present-day stress (~4.5 MPa) is more than double this long-term average, reflecting ~300 years of uninterrupted loading. This apparent stress excess may alternatively signal an incomplete rupture record: undocumented late Holocene earthquakes on Eastern Transverse Ranges structures (e.g., the Pinto Mountain, Blue Cut, or Chiriaco fault zones) could plausibly have imposed stress reductions of ~0.5-0.7 MPa per event, reconciling modeled stress with characteristic thresholds. Comparison with geodetic seismic moment accumulation (Mw potential ~7.6 for Carrizo, ~7.4 for Coachella) underscores fundamental differences between stress- and moment-based hazard metrics: stress evolution integrates multi-cycle rupture history and fault interactions, whereas moment accumulation reflects only elapsed time since the last event. These results demonstrate how physics-based stress models anchored by paleoseismic constraints can sharpen hazard interpretation and guide targeted paleoseismic investigations along the SAFS.

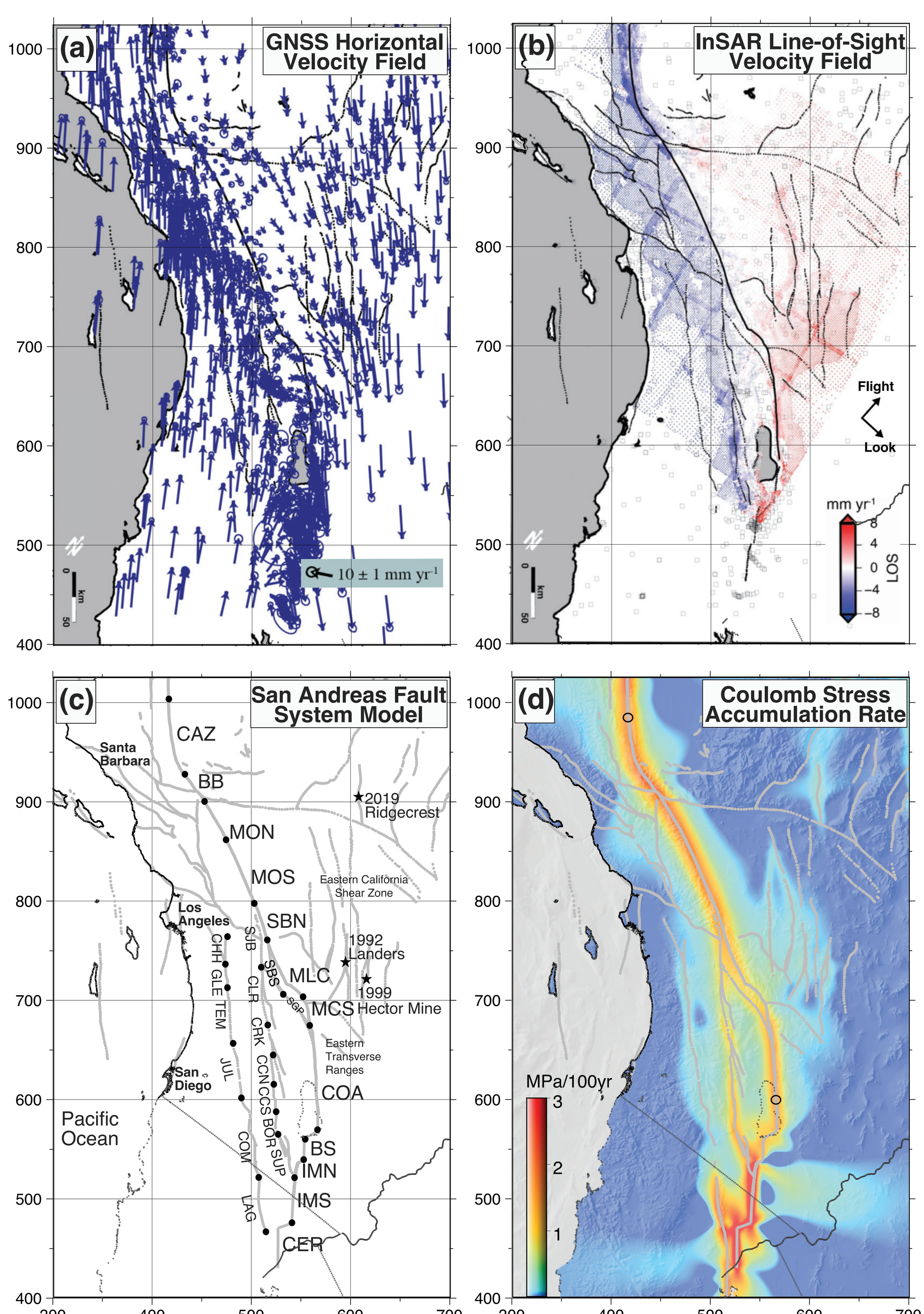

maxwell Earthquake Cycle Model

4D semi-analytic Fourier model (Smith & Sandwell, 2004; Sandwell & Smith-Konter, 2018)

- analytic calculations for depth and time-dependence
- numeric calculations for 2D Fourier transforms
- 4D deformation (t) = interseismic (deep slip) + Σ earthquakes (co. + postseismic)

Model efficiency

- 4096 x 4096 grid cells
- common locking depth, single event = 3s of CPU time
- 50+ depths, 100+ events over 1000 yrs = 18 mins

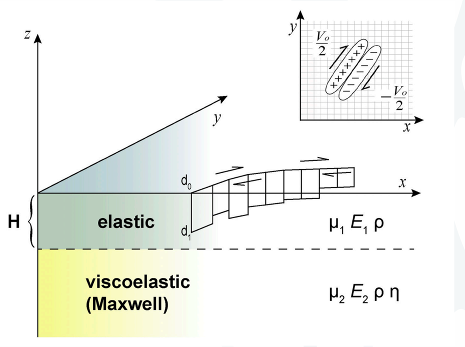

Coulomb Stress

To calculate Coulomb stress (τ_c), we incorporate the Coulomb failure condition

$$\tau_c = \tau_s - \mu_f \sigma_n$$

where μ_f is the coefficient of friction (0.6 for this study). Positive Coulomb stress indicates a tendency for failure (or stress accumulation) while negative Coulomb stress implies stress accumulation is not optimal.

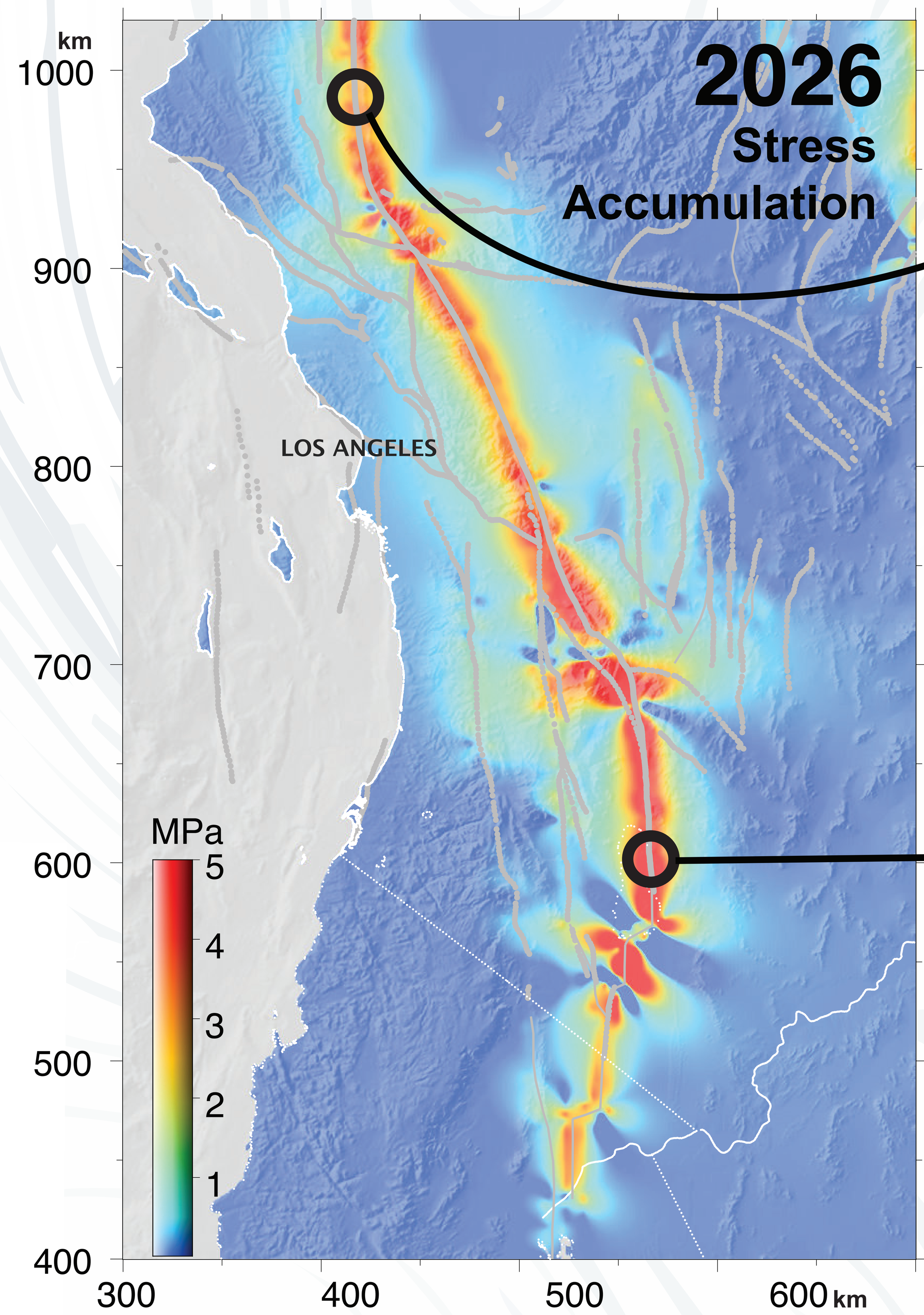

Central and southern San Andreas Fault System, geodetic data, and stress evolution model architecture:
(a) SCEC CGM GNSS horizontal velocity vectors and uncertainties.
(b) ALOS InSAR line-or-sight velocity data (Tong et al., 2013), where positive (red) velocities represent ground motion away from the satellite. Geodetic data analysis provided by Ward et al. (2021).
(c) San Andreas Fault System segment map used for this analysis. Black dots represent major fault segmentation.
(d) Modeled Coulomb stress accumulation rate per 100 yrs; stress is evaluated at 1/2 the locking depth of each segment. Open circles designate locations of stress evolution time-series results for the Carrizo and Coachella segments.

Paleoseismic Data

Calculations of accumulated stress over several earthquake cycles depend largely on the rupture history of the fault (Scharer & Yule, 2020) over the past few thousand years. However, there is little evidence that faults rupture periodically (Scharer et al., 2010) or at a uniform threshold (Murray & Segall, 2002).

Paleoseismic earthquakes of the San Andreas Fault System, like the 1812 and 1857 earthquake sequence along the southern SAFS, are demonstrative examples of this conundrum, with the M7.9 1857 rupture overlapping much of the proposed rupture lengths of the ~M7.5 1812 earthquake, yet with only 45 years of temporal separation.

We explore these issues with a 4D earthquake cycle stress accumulation model (Smith & Sandwell, 2004, Sandwell & Smith-Konter, 2018) using the present-day archive of geodetic and paleoseismic data (Scharer & Yule, 2020), as demonstrated in Burkhard et al. (2026).

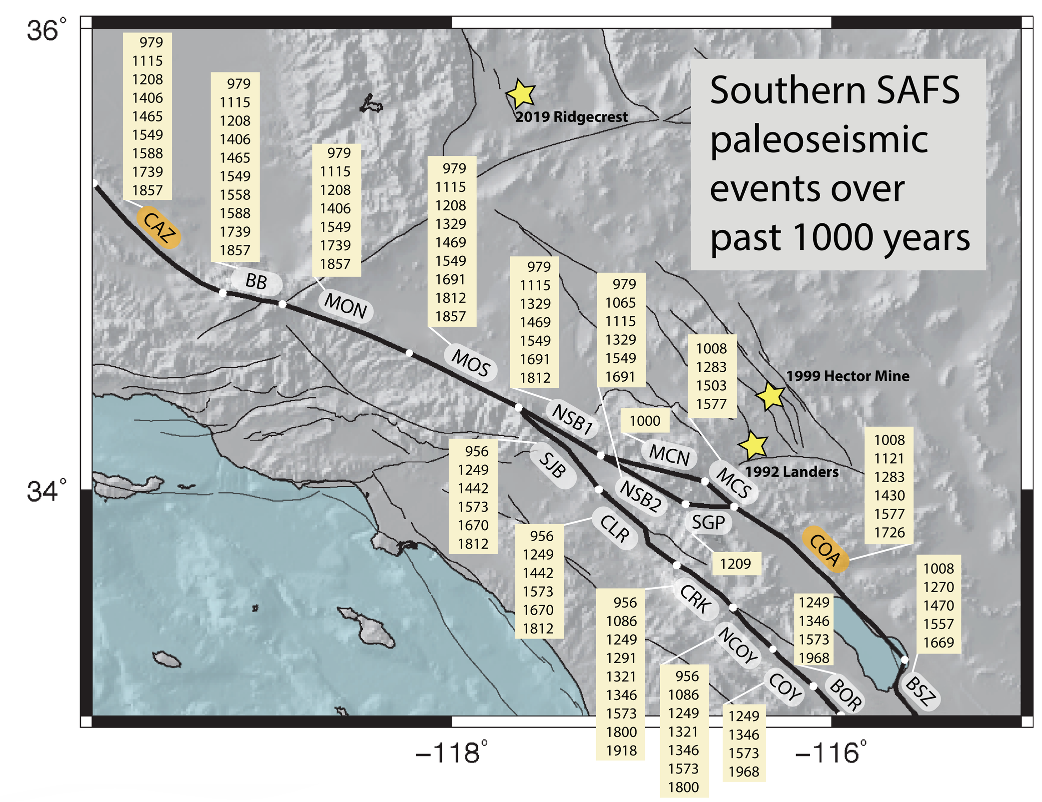

Open circles indicate locations of stress evolution time-series results for the Carrizo and Coachella segments:

Carrizo segment

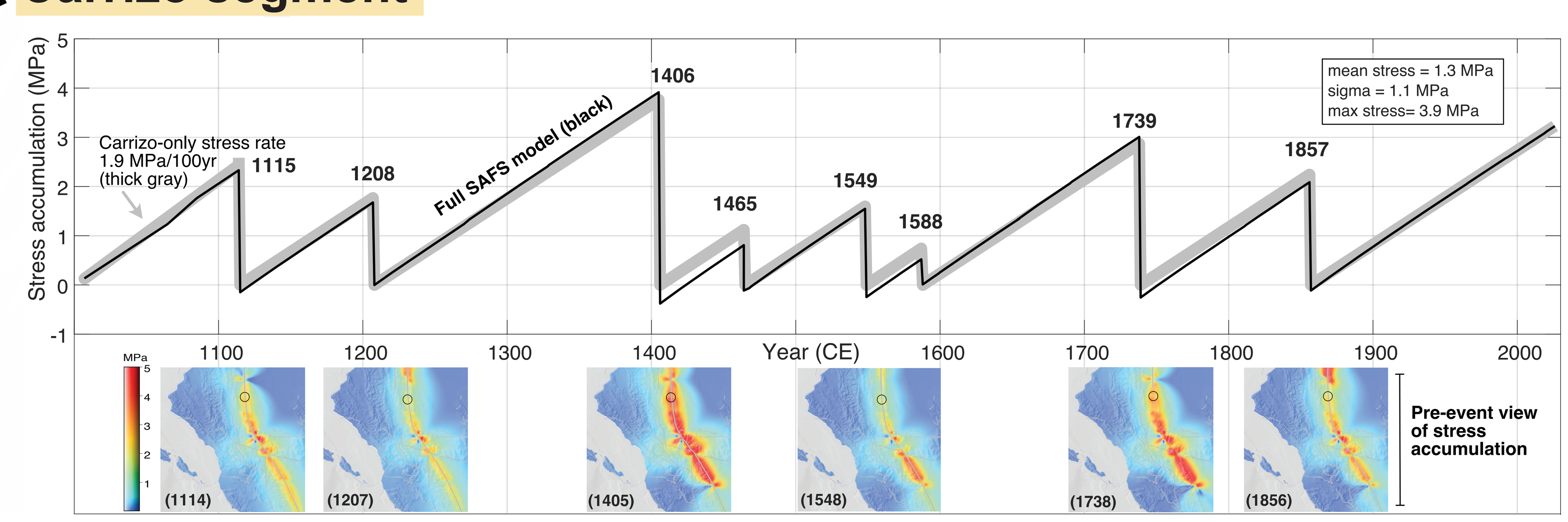

Coachella segment

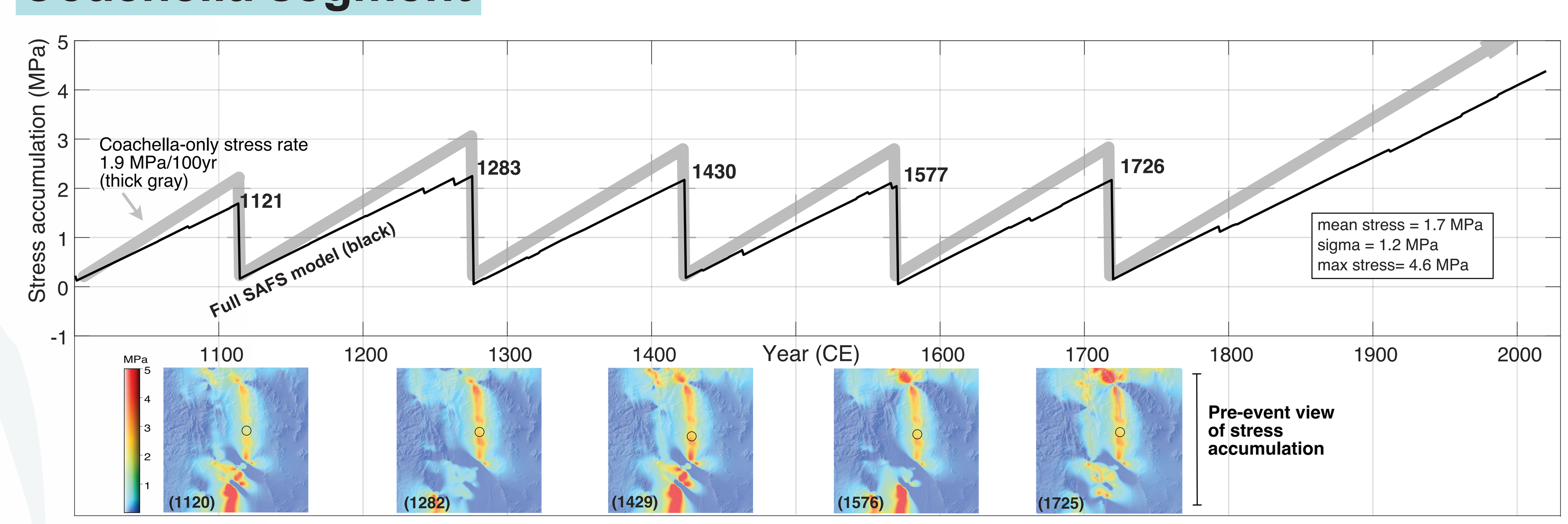

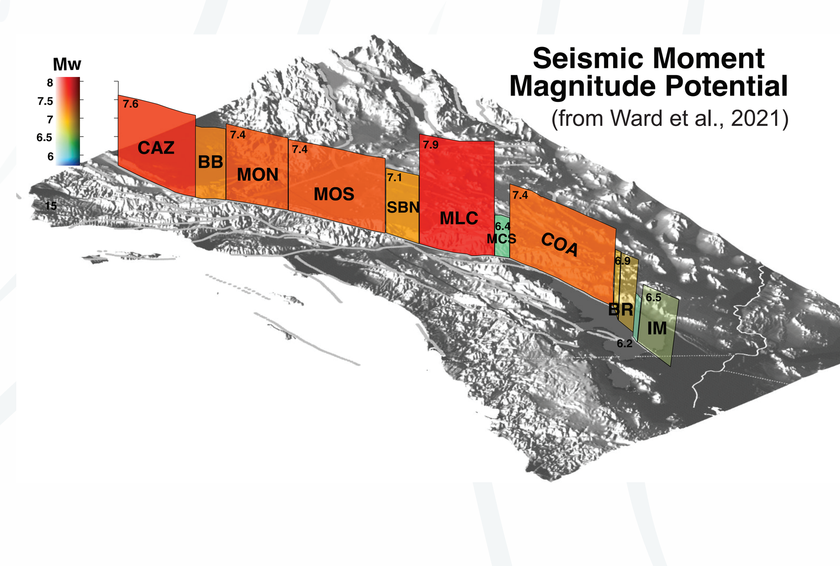

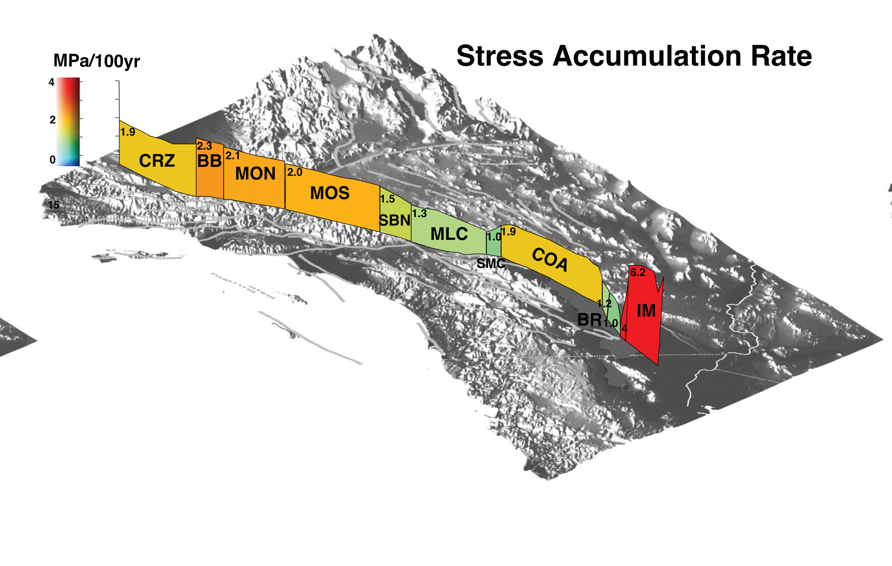

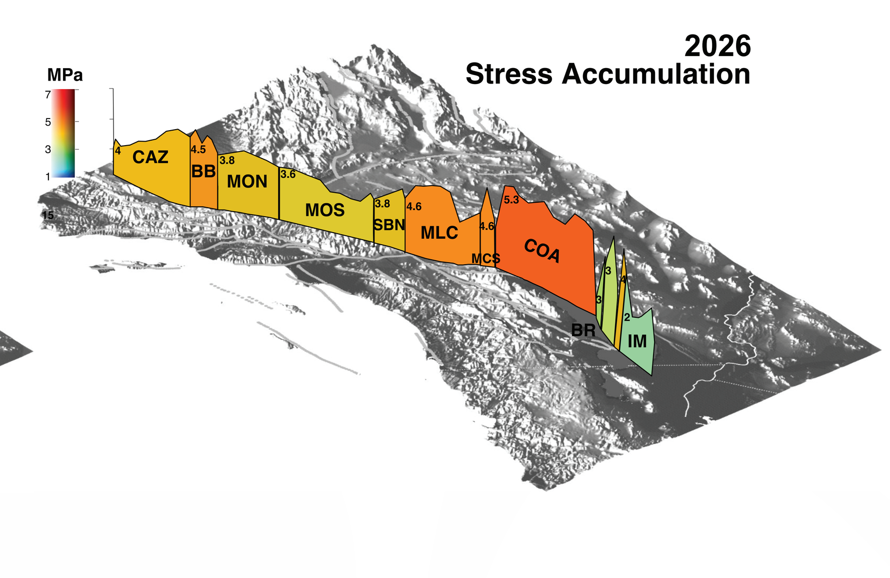

References

Burkhard, L. M. L., B. R. Smith-Konter, K. M. Scharer and D. T. Sandwell (2026), Cajon Pass and the southern San Andreas fault system: Earthquake cycle stress accumulation and present-day loading, JGR Solid Earth 131.

Murray, J. and P. Segall (2002), Testing time-predictable earthquake recurrence by direct measurement of strain accumulation and release, Nature, Vol. 419.

Sandwell, D. T. and B. R. Smith-Konter (2018), Maxwell: A semi-analytic 4D code for earthquake cycle modeling of transform fault systems, Computers and Geosciences.

Smith, B. R. and D. T. Sandwell (2006), A model of the earthquake cycle along the San Andreas Fault System for the past 1000 years, JGR, Vol. 111.

Smith, B. R. and D. T. Sandwell (2004), A three-dimensional semianalytic viscoelastic model for time-dependent analyses of the earthquake cycle, JGR, Vol. 109.

Scharer, K. M., G. P. Biasi, R. J. Weldon and T. E. Fumal (2010), Quasi-periodic recurrence of large earthquakes on the southern San Andreas fault, Geology, Vol. 38.

Scharer, K. M. and D. Yule (2020). A maximum rupture model for the southern San Andreas and San Jacinto faults, Geophys. Res. Lett.47, e2020GL088532.

Tong, X., D. T. Sandwell and B. R. Smith-Konter (2013), High-resolution interseismic velocity data along the San Andreas fault from GPS and InSAR, JGR Solid Earth 118.

Ward, L. A., B. R. Smith-Konter, X. Xu, and D. T. Sandwell (2021), Seismic moment accumulation response to lateral crustal variations of the San Andreas fault system, JGR Solid Earth 126.

SCEC Award 17169, 18149, 19161
2026 SCEC Annual Meeting
SCEC Contribution #15133